Hindawi
Journal of Chemistry
Volume 2019, Article ID 2403618, 10 pages
https://doi.org/10.1155/2019/2403618

Research Article

Preparation and Properties of Coal Ash Ceramic Membranes for Water and Heat Recovery from Flue Gas

Haiping Chen, Xiangsheng Li, Jiadi Wei, Yijun Feng, and Dan Gao

North China Electric Power University, School of Energy Power and Mechanical Engineering, National Thermal Power Technology Research Center, Beijing 102206, China

Correspondence should be addressed to Dan Gao; gaodan@ncepu.edu.cn

Received 22 July 2018; Revised 28 September 2018; Accepted 30 December 2018; Published 11 February 2019

Academic Editor: Yingchao Dong

In this paper, the manufacturing process of microceramic membrane is summarized. The main material of this membrane is fly ash which can reduce the sintering temperature and save the costs. The coal ash ceramic membrane (CACM) was characterized by XRD, SEM, and mercury intrusion method. The results show that the mullite phase formed by CACM at the sintering temperature of 1250°C has morphology and structural characteristics similar to the commercial microceramic membrane. The membrane surface is uniform and dense, without cracks; the pore diameter is 1–4 μm, and the porosity is 26.6%. Furthermore, the CACM and CMCM were compared at the aspects of water and heat recovery performance using flue gas. The experiment indicated that when the flue gas temperature was 50–85°C, the water recovery performance of these two kinds of membrane was similar. Also, the heat transfer capability of the coal ash ceramic membrane was close to that of the commercial microceramic membrane when the temperature range of flue gas was controlled between 50°C and 70°C. When the temperature of flue gas reaches 80°C, the heat transfer performance of the commercial ceramic membrane is better, and the difference of heat recovery between these two kinds of membranes is 19.3%. In general, the CACM and CMCM have similar mass transfer performance, and the heat transfer efficiency of CACM is lower than that of CMCM, but the costs of CACM is much lower than that of CMCM which has a good research prospect in the future.

1. Introduction

At of the end of March 2017, the installed capacity of China's 6000 kW and above power plants was 1.66 billion kilowatts, of which, thermal power was 1.08 billion kilowatts, accounting for 65.06%, which is still the main source of power supply in China [1]. The electric power development of the 13th Five-Year Plan requires the thermal power plants to further improve the policies and technologies for water and energy saving [2]. In recent years, water and energy saving work has made some benefits. But in 2014, Wei et al. [3] predicted that the increase rate of water consumption in power plants was still about 15%–20% over the next 20 years, with a huge increase in water consumption and an increase of at least 2.6 times in 2008. Now the energy is increasingly exhausted, and the energy consumption of thermal power is still huge, so the energy saving is an important key that must be taken seriously [4]. Water and energy conservation is a great challenge for the thermal power plants. In the thermal power plants, there is a large amount of water vapor and low-temperature waste heat in flue gas. Recovering water vapor and waste heat from flue gas can not only protect precious water resources but also improve thermal efficiency and reduce energy consumption.

In order to achieve the water and heat recovery from flue gas, besides several traditional technologies, more attention has been paid to the gas membrane separation technology in recent years. Choi et al. [5] introduced a thin-film composite hollow fiber membrane for laboratory-scale water vapor recovery experiments on real flue gas. The results showed that the maximum water flux and water vapor recovery efficiency reached 2.3 kg/m^{2}h and 27.7%, respectively. Reijerkerk et al. [6] reported that the highly hydrophilic, poly(ethylene oxide)-based block copolymers could remove CO_2 and water vapor from a ternary gas simulating flue gas in a postcombustion capture

configuration. Sijbesma et al. [7] developed composite hollow fiber membranes with a top layer of SPEEK and put twenty fiber bundles in artificial and real flue gas. Results showed that during a 150 h field test with the artificial flue gas, the fiber bundles continuously removed 0.6–1 kg/m^{2}h of water vapor; in addition, during the long-term field tests with real aggressive flue gas streams, an average water vapor removal rate of 0.2–0.46 L/m^{2}h was obtained during a continuous period of 5300 h. Chen et al. [8] studied the properties of SPEEK/PES that was a hydrophilic composite hollow fiber membrane and experimented by using the simulated flue gas. The research indicated that the water recovery rate increased with the temperature (40–70°C). When the sulfonation degree of SPEEK was 59%, the water vapor permeation flux could be up to 12.7494 g/m^{2}h.

In the past few years, membrane processes have received great attention and extensively developed on gas and liquid separation processes. One of the limitations for a massive industrial penetration of the membrane is the lack of suitable membrane materials that can withstand harsh industrial conditions for extended periods of time [9]. This is because most membrane materials that have been commercialized so far are polymers. Compared with the organic membrane, the inorganic porous ceramic membrane has some outstanding advantages that organic membrane does not have, such as great thermal stability, high mechanical strength, acid and alkali resistance, long life span, and so on. Zou et al. [10] proposed a novel process for the preparation of a low-cost fly ash based a cosintering process. In the novel process, the microfiltration layer was sprayed on fly ash carrier, and mullite fiber was added to reduce cosintering differences. The average pore size of the prepared ceramic film was 100 nm, with a high permeability of 450 ml^{-2} h^{-1} bar^{-1}. Zhu et al. [11] used a finger-like and sponge-like mullite hollow fiber made of fly ash to produce a low-cost multilayer mullite-titanium dioxide composite ceramic hollow fiber microfiltration membrane. It is found that the composite membrane achieved a 97% TOC removal efficiency in 200 mg·L^{-1} synthetic (oil/water) emulsion. Song et al. [12] prepared a ceramic membrane with a higher filtration efficiency and better regeneration performance than a membrane made of alumina powder by using short fibers as a starting material.

And it is more widely researched and more suitable to recover water and heat from flue gas [13–19]. Gas Technology Institution (GTI) developed a transport membrane condenser (TMC) which was made from porous ceramic membrane tube bundles. The technology had achieved good heat and water recovery performance, the water recovery rate was equal or larger than 40% recovery, and the increase of efficiency was more than 5% [20–24]. Bao et al. [25] carried out experiments to study the phenomena for both a porous ceramic membrane tube bundle and an impermeable stainless steel tube bundle with the same characteristic dimensions. It was found that the condensation rate for the porous ceramic membrane tube bundle increased by 60–80% compared with that of the stainless steel tube bundle. Wang et al. [26] used a tubular ceramic membrane as the transport membrane condenser for water vapor and heat recovery from flue gas and studied the effects of several important operational parameters on the process performance in terms of mass and heat transfer across the membrane. Results indicated that 20–60% water recovery and 33–85% heat recovery were achievable when using cold water as the coolant. Zhou et al. [27, 28] presented the application of a 20 nm pore-sized porous ceramic membrane for condensation heat transfer in artificial flue gas and investigated the phenomenon of capillary condensation. The study showed that the water recovery rate of the module could be up to above 80% and the heat recovery efficiency could be up to above 40%.

However, due to expensive raw materials of commercial inorganic porous ceramic membrane, complicated fabrication process, and rigorous sintering temperature, the production cost and the selling price are quiet high and both development and application of the inorganic porous ceramic membrane are greatly restricted. Consequently, the new low-cost, excellent performance membrane preparation research is also a major point in the application of gas membrane separation technology to recover water vapor and waste heat from flue gas.

Coal ash is the main solid waste discharged by thermal power plants, and the amount of fly ash is increasing year by year. If most fly ash is not disposed properly, it will pollute the atmosphere and do harm to the human. The main oxides include SiO_2 and Al_2O_3, accounting for more than 60%, which are also the main components of CMCM [29]. Therefore, except controlling the environmental pollution greatly, consequently, the preparation cost of ceramic membranes would reduce significantly by reusing coal ash as the main raw materials to fabricate the new type of tubular ceramic membrane.

The application of fly ash is mostly focused on cement concrete production, soil improvement, sewage treatment, construction engineering, and other fields [30–38]. There are relatively few studies on the elaboration of porous ceramic membranes by fly ash. Cao et al. [39] used waste fly ash and natural bauxite, with AlF_3 and V_2O_5 as additives to prepare mullite ceramic membrane supports and found that the membrane support with 4 wt.% AlF_3 and 3 wt.% V_2O_5 (A_4V_3) had the best performance. Dong et al. [40] prepared cordierite-based porous ceramic microfiltration membranes by using fly ash and basic magnesium carbonate as starting materials and confirmed that α-cordierite was formed above 1100°C and its crystallinity improved steadily with further increasing firing temperature. Wu et al. [41] developed mullite-based ceramic proppants with low density and high strength by using fly ash, bauxite, clay, and composite mineralizers. They investigated the phase composition and microstructure at different sintering temperatures and found that at the best sintering temperature of 1370°C, the acid solubility was 5.7% and the crushing rate was 5.0% under 52 MPa. Fang et al. [42] made crack-free tubular supported ceramic microfiltration membranes using refined fly ash as the raw material by a slip-casting method and found that the pore-size distribution of the membrane became narrower by applying a second coating. Liu et al. [43] reused coal ash to fabricate anorthite-cordierite-based porous ceramic membrane supports by using dolomite

and characterized the membrane. Results indicated that adding dolomite could adjust the support pore-structure, inhibiting the sintering of coal ash while providing acceptable mechanical strength, and form more anorthite and cordierite with good thermal properties in the porous membrane support materials.

Although the ceramic membrane separation technology and the preparation of the low-cost ceramic membrane by fly ash have been researched, there was no comparison between the CACM and CMCM about the water and heat recovery performance in flue gas. In this paper, the main research content was to prepare and characterize microsized ceramic membranes by coal ash (Hohhot, Inner Mongolia Province, China) as major materials and perform contrast experiments on water and heat recovery performance between the two kinds of membranes. In this way, the issue on the feasibility of CACM replacing CMCM for the water and heat recovery from flue gas has been further investigated.

2. Preparation and Characterization

2.1. Preparation of Coal Ash Ceramic Membrane. In this paper, fly ash is selected as the main raw material to prepare the microceramic membrane. The main preparation process is shown in Figure 1. Detailed preparation process is as follows:

(1) Fly ash screened from a 60 mesh screen and kaolin, dextrin, technical-grade carboxymethyl cellulose (CMC), and other ceramic additives was mixed in a design ratio and stirred for 5 minutes.

(2) The mixture in the beaker was placed in a vertical ball mill (XQM-20, Changsha Tencan Powder Technology Co., Ltd) for power and dry milling for 4 hours to ensure uniform mixing of the ingredients.

(3) Appropriate amount of distilled water that meets the requirements was added to the mixture and mixed in the mixer (HL-5, Henan Xin Long Machinery Factory).

(4) The mixture was stirred 4-5 times with the vacuum mixer (S-48, Henan Xin Long Machinery Factory) and sealed at 30°C for 12 hours, and then the material was mixed 2-3 times again.

(5) The blank (i.e., the mixture having certain plasticity) was extruded with a screw extruder (LWJ63, Henan Xin Long Machinery Factory) and straightened on a straightener (XZJ-25/1000, Henan Xin Long Machinery Factory) for 48 hours.

(6) Sintering in a high-temperature tubular electric furnace (TSK-8-14, FuEnSen (Beijing) Dianlu Co., Ltd), and the heating rate was set to 2-3°C/s and kept warm for 30 min at 135°C to make the prepared membranes dry and to remove free water. Then, the prepared membranes were insulated for 120 min at 325°C to remove bound water and stayed warm for 240 min at 750°C to remove organic additives and pore-forming agents. At last, it was fired at 1250°C for 300 min and cooled inside the furnace.

2.2. Membrane Performance Characterization

2.2.1. Microscopic Morphology. In Figure 2, the scanning electron microscopy (SEM) pictures of α-Al_2O_3 microceramic membrane (Beijing Hongzhijiahe Technology Co., Ltd.) and coal ash ceramic membrane (CACM) are captured by JSM6490LV SEM (JEOL Electronics Corporation).

Figure 2 shows the morphology of the α-Al_2O_3 microceramic membrane and the coal ash ceramic membrane at 100 and 1000 magnifications of SEM, respectively. It can be seen that the single grain of all the samples has an irregular shape. Figure 2(a) presents that the surface of CMCM is not smooth and there are tiny irregular protrusions. Compared with Figure 2(b), the existence of small holes can be more clearly observed. Figure 2 shows that both CACM and CMCM are compact and have no defects, and the surface pore diameter can be clearly found to be distributed between 1 micrometer and several micrometers. Compared to CMCM, there are more microsized particles on the surface of CACM. It is caused by a different processing technique.

2.2.2. Pore-Size Distribution and Porosity. The pore size test of the two kinds of membranes is performed by the mercury intrusion method (Quantachrome Instruments Trading (Shanghai Co., Ltd)) and the porosity is calculated; the results are shown in Figure 3 and Table 1.

2.2.3. Phase Composition by XRD. The main components of the two membranes are tested and analyzed by XRD (AL-Y300, Dandong Aolong Ray Instrument Group Limited Company), as depicted in Figure 4.

The XRD analysis shown in Figure 2 indicates that the main composition of commercial α-Al_2O_3 microceramic membrane is corundum (PDF#46–1212); both corundum and mullite (PDF#15–0776) exist in the coal ash ceramic membrane, but mullite is the majority. So there are some performance differences between CACM and CMCM. Based on the impacts of corundum and mullite on thermal conductivity of the membrane, theoretically, it can be predicted that thermal conductivity of the commercial membrane is better than that of the prepared ceramic membrane under fixed conditions during the water and heat recovery process [44, 45].

3. Experimental Apparatus and Methods

3.1. Experimental Apparatus. The experiment system is presented in Figure 5. In this system, all the pipes and tanks are thermally insulated using cotton, and the outside of the module is also heat insulated. All temperatures are measured by a temperature sensor (PT100) inside the pipe and monitored by a digital temperature indicator. The relative humidity of gas is measured by a humidity transmitter (VAISALA, HMT3307). The amount of water recovery is obtained by the difference in the mass of the water vapor contained in the inlet and outlet of the component, where the drying pipe is used to measure the water vapor not absorbed by the component.

Considering the main composition of flue gas, in order to simplify the experimental operation, this study uses the

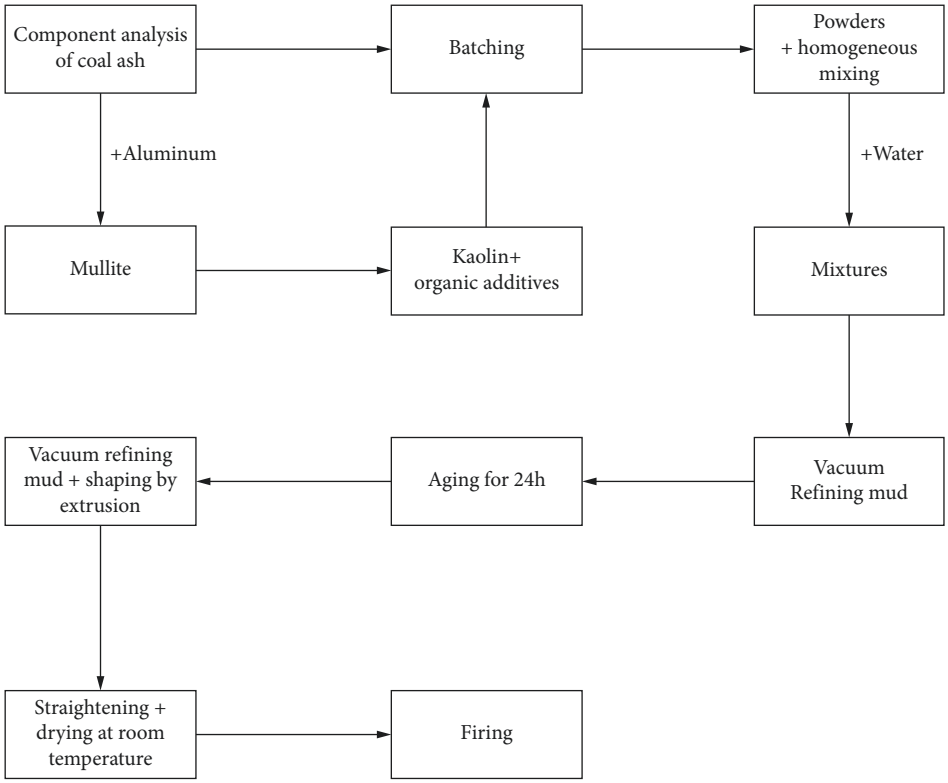

Figure 1: Flow chart for preparation of coal ash ceramic membrane.

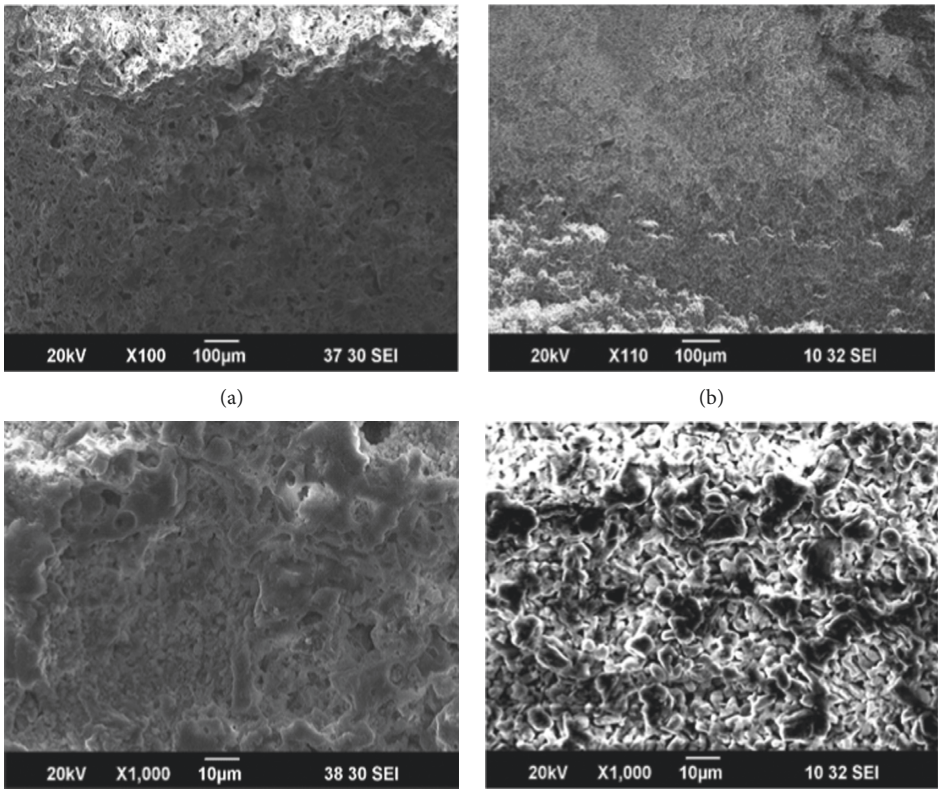

Figure 2: SEM pictures of the cross section of ceramic membranes: (a) α-Al_2O_3 microceramic membrane (size scale: 100 μm); (b) coal ash ceramic membrane (size scale: 100 μm); (c) α-Al_2O_3 microceramic membrane (size scale: 10 μm); (d) coal ash ceramic membrane (size scale: 10 μm).

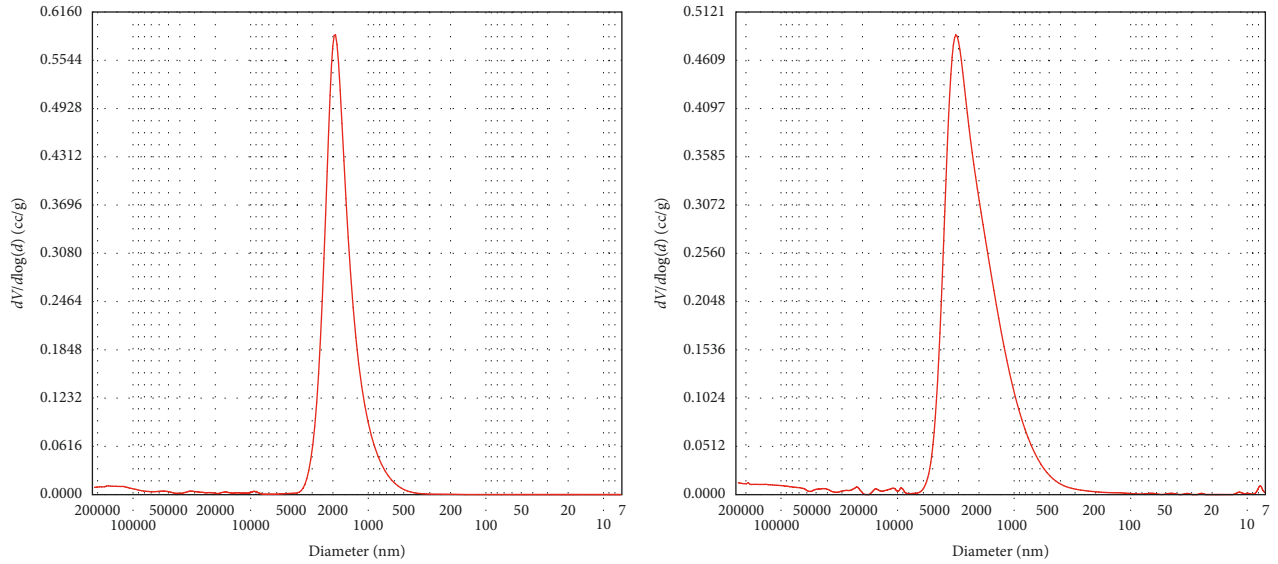

Figure 3: Pore-size distribution of the two membrane: (a) α-Al_2O_3 microceramic membrane; (b) coal ash membrane.

Table 1: Comparison of pore-size distribution and porosity.

	Major pore-size distribution	Porosity
Coal ash ceramic membrane	1–4 μm	26.6%
α-Al_2O_3 microceramic membrane	1–3 μm	27.2%

artificial gas which consists of nitrogen, water vapor, and a certain proportion of carbon dioxide. Nitrogen is supplied by two pure gas cylinders, the gas in the left one is fed by an FC (mass flow controller) to the gas buffer tank, then to the humidifier in order to supply the saturated mixed gas, and the middle and right gas cylinders provide dry nitrogen and carbon dioxide, respectively. Balancing the flow rates of the three streams by their respective FCs, the final relative humidity, and the gas ratio of the gas supplied to the module can be controlled.

The module shell (i.e., membrane tube outside) is connected to the cooling water system, which the water tank contains a heating resistance wire, and the external insulation provides a certain temperature and a stable flux of water. In addition to the water tank in the cooling water system, the most important component is the water pump. For one thing, it keeps the cooling water in a stable circulating flow to continuously remove the water and heat in the artificial flue gas, and for another, it provides the pressure difference inside and outside of the ceramic membrane tube to form pressure driving force.

The experimental operating conditions in the experiments are shown in Table 2.

3.2. Methods. In the module, the heat and water recovery using ceramic membrane is actually a complex process of heat and mass transfer. In order to measure the difference in heat and mass transfer performance between CACM and CMCM, two kinds of ceramic tubes with the same length (i.e., 0.8 m) were used for control variable experiment in this paper.

The method is to calculate the amount of water recovery under each working condition, which is the amount of recovered water per unit hour and unit area. The water recovery rate is the ratio that the recovered water of a single ceramic membrane is divided by the water vapor in the inlet feed gas.

The amount of recovered water can be calculated as

$$J_{\text{rev}} = \frac{\left(M_{\text{c,out}} - M_{\text{c,in}}\right)}{A_{\text{i}}}. \quad (1)$$

The amount of nitrogen passing through the membrane and the heat loss of the module are ignored, and in most cases, the amount of water recovered is negligibly small compared to the amount of cooling water, so the heat balance in the module can be simplified to

$$M_{\text{c,out}} - M_{\text{c,in}} = M_{\text{v,in}} - M_{\text{v,out}}. \quad (2)$$

The water recovery rate is the ratio of the recovered water mass flow to the inlet water vapor mass flow:

$$\eta_{\text{rev}} = \frac{\left(M_{\text{v,in}} - M_{\text{v,out}}\right)}{M_{\text{v,in}}} \times 100, \quad (3)$$

where J_{rev} is the amount of recovered water per unit minute and unit area (i.e., the permeate water flux through the membrane); $M_{\text{c,in}}$ and $M_{\text{c,out}}$ are the mass flow rate of the inlet and outlet cooling water, respectively; $M_{\text{v,in}}$ and $M_{\text{v,out}}$ are the mass flow rate of water vapor in the inlet and outlet feed gas, respectively; A_{i} is the inner surface area of the membrane; η_{rev} is the water recovery rate.

The flow of flue gas and cooling water inside and outside the ceramic membrane tube is arranged in a downstream flow, and the reduced heat of the flue gas is transferred to the cooling water during the flow process, leading to the

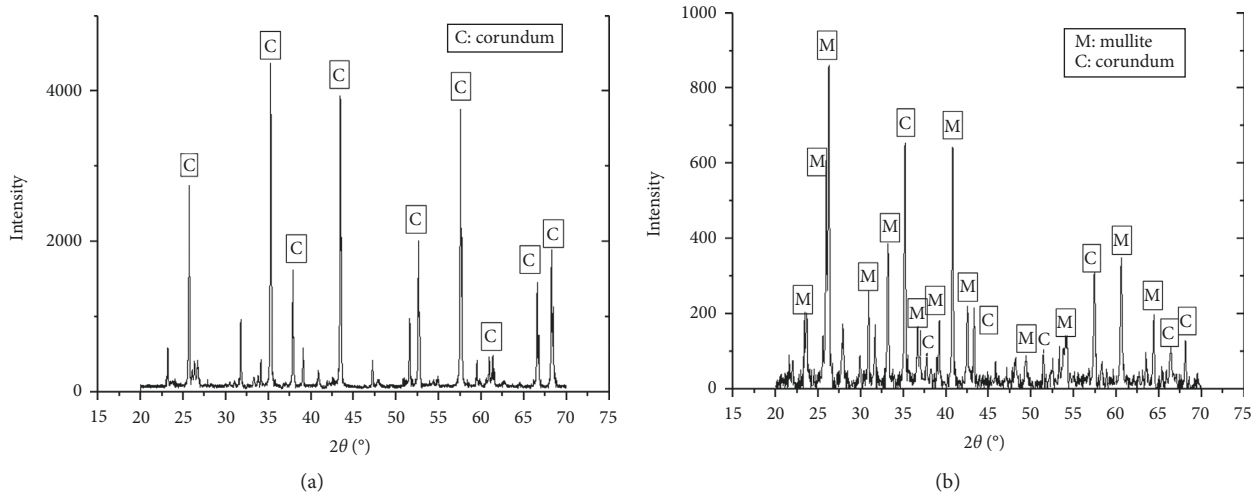

Figure 4: X-ray diffraction patterns of ceramic membranes. (a) X-ray diffraction pattern of the α-Al_2O_3 microceramic membrane. (b) X-ray diffraction pattern of the coal ash ceramic membrane.

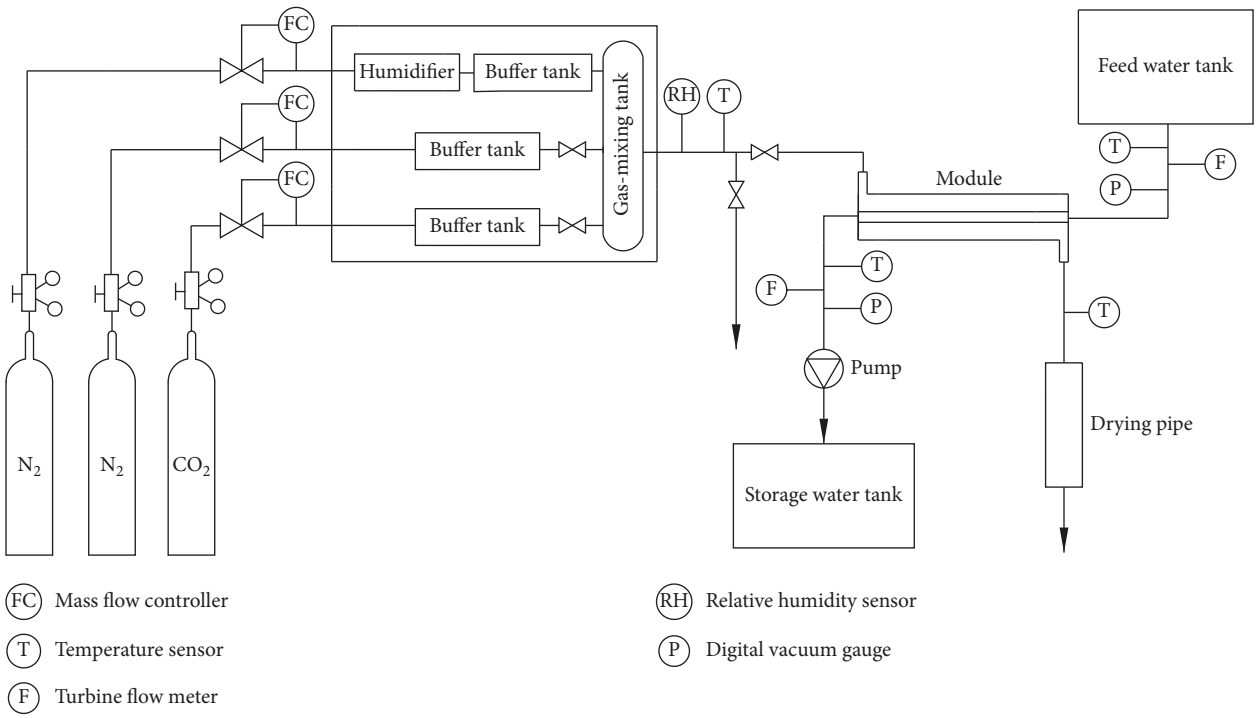

Figure 5: Schematic of experimental apparatus.

temperature rise of the cooling water. The temperature difference between the inlet and outlet cooling water can be used to evaluate the heat transfer performance of the experiment system, which is calculated by the following equation:

$$\Delta t = t_{c,out} - t_{c,in}. \quad (4)$$

4. Results and Discussion

4.1. Comparative Analysis on Permeability of Two Kinds of Ceramic Membranes. The water recovery performance and water recovery of the two membranes were controlled at an experimental temperature of 50–85°C. In the experiment, the total flow rate of the feeding gas was controlled at 6 L/min. Through adjusting the flow rates of dry nitrogen and wet nitrogen, a different relative humidity is obtained and feed gas is controlled to be under saturated state or unsaturated, specifically wet + dry: 6 + 0 L/min and wet + dry: 3 + 3 L/min, as shown in Figures 6 and 7.

Figure 6 describes that, in the whole experimental temperature range, no matter if the water vapor of the feed gas is in the saturated or unsaturated state, the water permeability of the CACM is similar to the commercial α-Al_2O_3 microceramic membrane. And the water permeability of

Table 2: Experimental operating conditions.

Name	Contents
Ceramic membranes	ID/OD: 0.08/0.12 m; length: 0.8 m; α-Al_2O_3 microceramic membrane; coal ash ceramic membrane
Module	ID/OD: 0.415/0.455 m; length: 0.8 m; 304 stainless steel
Feed gas	N_2; H_2O; CO_2
Feed gas flux	6 L/min
Feed gas temperature	50–85°C
CO_2 volume fraction	0–20 vol.%
Cooling water flux	1 L/min
Cooling water temperature	28°C

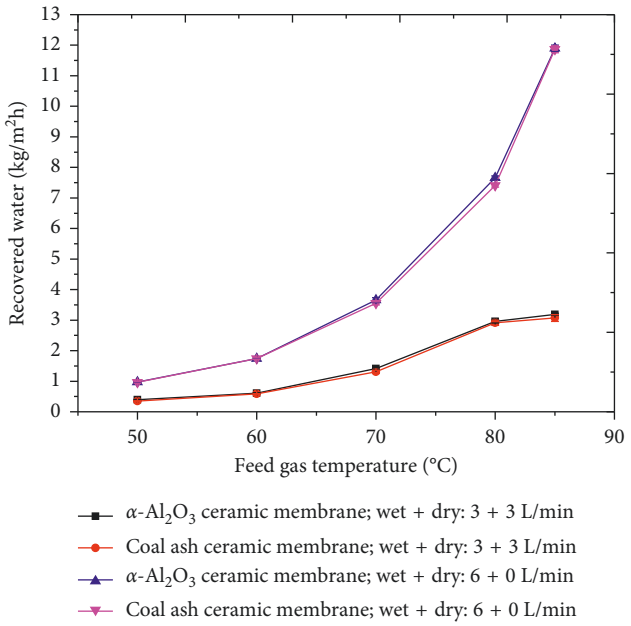

Figure 6: Comparison of recovered water.

the two membranes both increase with the rise of feed gas temperature. Furthermore, under the unsaturated condition, the higher the feed gas temperature, the slower the growing rate of the water recovery. However, in the case of saturation, the growing rate of water recovery enhances more sharply under higher feed gas temperature. The similar result is also reflected in Figure 7. It is found that the water recovery rate increases with the rising temperature of the feed gas under saturated condition. Under the opposite condition, the water recovery rate gets larger first and then decreases. At the same inlet flow rate, the water recovery rate of the saturated water vapor is higher than that of the unsaturated water vapor.

The results show that when the temperature of flue gas is 50–85°C, both CACM and CMCM can effectively recover the moisture in the flue gas, especially when the water vapor of the feed gas is saturated, the difference between them is small, and more water vapor can be recovered from the flue gas more effectively. Therefore, the membrane recovering the water vapor from flue gas is more suitable to install and use after desulfurization.

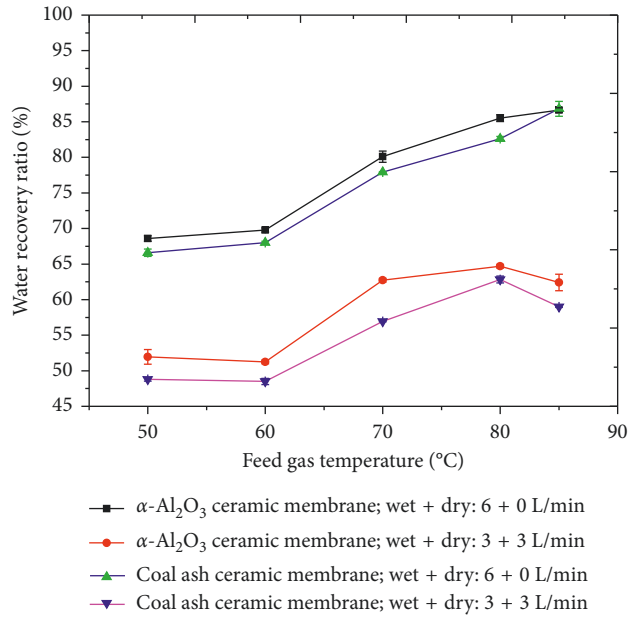

Figure 7: Comparison of water recovery rate.

4.2. Effect of CO_2 in Feed Gas on the Membrane Performance. Considering that the content of carbon dioxide in the flue gas has reached 10% or more besides nitrogen and water vapor, the carbon dioxide is introduced into experiment to study the effect of carbon dioxide on the water recovery performance of the feed gas. The result is shown in Figure 8.

Figure 8 shows that the three curves of 10–20% volume CO_2 and without CO_2 experimental gas substantially coincide when the simulated flue gas temperature range is 50–85°C. The result shows that the carbon dioxide in the flue gas has little effect on the recovery of water from the ceramic membrane tube.

Therefore, it is feasible to use a simplified binary gas system (nitrogen and water vapor) instead of real flue gas to study the recovery of water vapor in flue gas by ceramic membrane.

4.3. Heat Recovery and Temperature Rise of Cooling Water. The heat recovery by the ceramic membrane is divided into three parts: the heat between the feed gas and the cooling water including the convective sensible heat, the latent heat of condensation, and the heat carried by the recovered water vapor. They are shown in Figure 9.

Figure 9 shows that the temperature rise of cooling water both the coal ash ceramic membrane (CACM) and the commercial microceramic membrane (CMCM) increases with the growth of the feed gas temperature, and the promotion will become more obvious as the growth of temperature. Both membranes have a commonality. When the feed gas is in the saturated state, the temperature rise is faster than that in the unsaturated state, as the feed gas temperature increases. The difference of coal ash ceramic membrane is more obvious. When the temperature of feed gas is 50–70°C, the difference of the heat transfer between CACM and CMCM is not obvious, and when the temperature

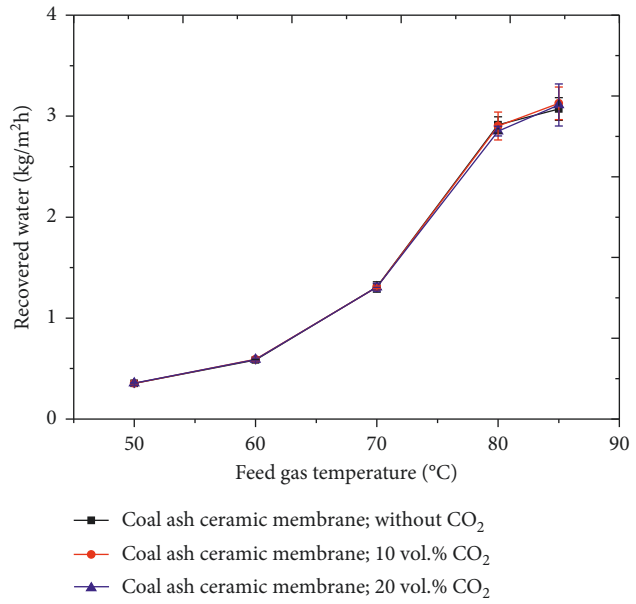

Figure 8: The influence of CO_2 content in feed gas on the water recovery.

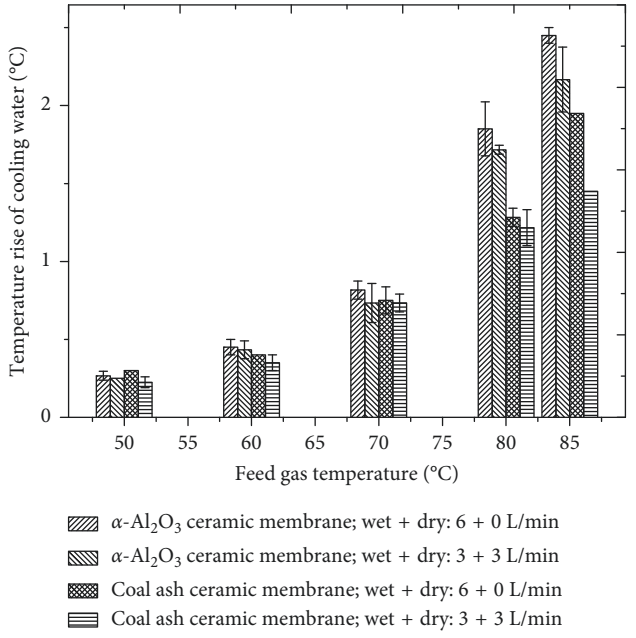

Figure 9: Comparison of temperature rise of cooling water between the two membranes.

reaches 80°C, the cooling water temperature rise of CMCM is about 1°C higher than CACM.

However, the study of higher feed gas temperature is not carried out, considering the low-temperature and saturated gas exhausted from flue gas desulfurization (FGD) in coal-fired power plants. So the study for saturated flue gas in this range of temperature has guiding significance for practical application.

In general, the heat transfer capacity of CMCM is close to CACM at 50–70°C. When the feed gas temperature reaches 85°C and is saturated, the difference in heat transfer performance between the coal ash ceramic membrane and the commercial microceramic membrane is obvious. The cooling water temperature rise of CMCM is 2.43°C, and the temperature rise of CACM reaches 1.96°C. The percentage difference in heat recovered from the flue gas is 19.3%. This is because that the main component of CMCM is corundum, whose thermal conductivity and porosity (porosity given in Table 2) are higher than the main component (i.e., mullite) of CACM. When the ceramic membrane is used to recover heat and water of flue gas, the water vapor mainly condenses on the outer surface and penetrates the membrane by liquid form. The heat transfer performance depends mainly on the thermal conductivity and porosity of the ceramic membrane [43, 44]. The experimental results are also consistent with the conclusions in [28] for studying the heat and mass transfer of microceramic membranes.

The experimental uncertainties can be originated from the temperature and the measurements of cooling water flow rate which also involves the precision of the thermocouple, humidity transmitter, and flow meter. The propagation of uncertainties in terms of the experimental parameters can be calculated by the following differential equation:

$$\eta_x = \sqrt{\left(\frac{\partial f}{\partial u}\right)^2 \eta_u^2 + \left(\frac{\partial f}{\partial v}\right)^2 \eta_v^2 + \left(\frac{\partial f}{\partial w}\right)^2 \eta_w^2 + \ldots}, \quad (5)$$

where the subscript x is a function of the independent variables, such as u, v, and w. The uncertainties of the measured parameters are listed in Table 3. The calculated results are as follows: the uncertainty of the mass flux is $\pm 0.141\ \mathrm{kg/m^2h}$, the maximum uncertainty of the temperature rise of cooling water is ±0.15°C, and the maximum uncertainty of efficiency of permeation is ±1.71%.

5. Conclusion

In this paper, the coal ash ceramic membrane was prepared and characterized, and the comparison experiments between coal ash ceramic membrane and commercial microceramic membrane were carried out to study the difference in water recovery and heat transfer performance in artificial flue gas. The main conclusions are drawn as follows:

(1) The sintering temperature of the coal ash ceramic membrane is 1250°C, far lower than 1700°C, which is the sintering temperature of the commercial ceramic membrane [46]. Lower sintering temperature could reduce the production costs significantly.

(2) It was found that the mullite phase formed at the sintering temperature of 1250°C had morphology similar to that of the commercial microceramic membrane surface, and the surface was uniform and dense without cracks, and the pore diameters were 1–4 μm. The porosity of the fly ash ceramic membrane was 26.6%, which was only 0.6% inferior

Table 3: Experimental uncertainties.

Property	Uncertainty	Range
Feed gas temperature	0.1°C	50–85°C
Coolant flow rate	0.1 L/min	6 L/min
Inlet coolant temperature	0.1°C	23.9–24.4°C
Outlet coolant temperature	0.1°C	24.5–26.8°C

to that of the commercial microceramic membrane. The permeability of these two ceramic membranes is similar.

(3) When the feed gas temperature was 50–85°C, the amount of recovered water when feed gas was in the saturated state or the unsaturated state was approximately the same. When the feed gas was in the unsaturated state, the recovery water rate of coal ash ceramic membrane was a little higher than the commercial microceramic membrane. Considering the actual conditions of feed gas (being saturated before passing through components and becoming unsaturated after passing through them), coal ash ceramic membrane was more suitable for installation and used after the desulfurization device.

(4) In the comparative experiment of evaluating the heat recovery performance of membrane, the heat transfer capacity of coal ash ceramic membrane was close to commercial microceramic membrane when the feed gas was at 50–70°C. When the temperature of the feed gas reached to 80°C, the heat transfer performance of commercial ceramic membrane is slightly better than that of the coal ash ceramic membrane because of the difference of materials and ceramic membrane porosity between the coal ash and commercial microceramic membrane.

Nomenclature

J: Flux (kg/m^{2}h)
M: Mass flow rate (kg/h)
A: Area (m^2)
η: Efficiency (%)
t: Temperature (°C)
i: Inner diameter of tube
rev: Recovered water
c: Cooling water
in: Inlet
out: Outlet
v: Water vapor
Δt: Temperature difference.

Data Availability

The data used to support the findings of this study are available from the corresponding author upon request.

Conflicts of Interest

The authors declare that there are no conflicts of interest.

Acknowledgments

This work was funded by the project National Key R&D Program of China (grant no. 2018YFB0604301), the Fundamental Research Funds for the Central Universities (grant no. 2015ZZD11), and the North China Electric Power University's Double First-Rate Guides Special Top Innovative Talents Cultivation (grant no. XM1805311).

References

[1] CEC, *Statistic of China Power Industry March 2018*, Planning and Development Division of China Electric Council, Beijing, China, 2018.

[2] W. Pan, Z. Liu, and B. Zhang, "Analysis of current status of thermal power saving in China and suggestions for measures," *China Electric Power*, vol. 50, no. 11, pp. 158–163, 2017.

[3] G. Wei, L. Xing, J. Meng et al., "Prediction of water consumption in thermal power generation in China and analysis of water saving technology development (in English)," *Proceedings of the CSEE*, vol. 34, no. 32, pp. 5717–5727, 2014.

[4] C. Wu, "Analysis of energy saving and consumption reduction measures in thermal power plants," *Low Carbon World*, vol. 1, no. 1, pp. 43-44, 2017.

[5] O. Choi, P. G. Ingole, and H. K. Lee, "Preparation and characterization of thin film composite membrane for the removal of water vapor from the flue gas at bench scale," *Separation and Purification Technology*, vol. 211, pp. 401–407, 2019.

[6] S. R. Reijerkerk, R. Jordana, K. Nijmeijer, and K Wessling, "Highly hydrophilic, rubbery membranes for CO_2, capture and dehydration of flue gas," *International Journal of Greenhouse Gas Control*, vol. 5, no. 1, pp. 26–36, 2011.

[7] H. Sijbesma, K. Nymeijer, R. V. Marwijk, R. Heijboer, J. Potreck, and M. Wessling, "Flue gas dehydration using polymer membranes," *Journal of Membrane Science*, vol. 313, no. 1, pp. 263–276, 2008.

[8] H. Chen, Y. Zhou, J. Sun et al., "An experimental study of membranes for capturing water vapor from flue gas," *Journal of the Energy Institute*, vol. 91, no. 3, pp. 339–348, 2017.

[9] D. Koutsonikolas, S. Kaldis, and G. P. Sakellaropoulos, "A low-temperature CVI method for pore modification of sol–gel silica membranes," *Journal of membrane science*, vol. 342, no. 1-2, pp. 131–137, 2009.

[10] D. Zou, M. Qiu, X. Chen, E. Drioli, and Y. Fan, "One step co-sintering process for low-cost fly ash based ceramic microfiltration membrane in oil-in-water emulsion treatment," *Separation and Purification Technology*, vol. 210, pp. 511–520, 2019.

[11] L. Zhu, M. Chen, Y. Dong, C. Y. Tang, A. Huang, and L. Li, "A low-cost mullite-titania composite ceramic hollow fiber microfiltration membrane for highly efficient separation of oil-in-water emulsion," *Water Research*, vol. 90, pp. 277–285, 2016.

[12] X. Song, B. Jian, and J. Jin, "Preparation of porous ceramic membrane for gas-solid separation," *Ceramics International*, vol. 44, no. 16, pp. 20361–20366, 2018.

[13] G. Chen, Q. Hong, W. Xing, and N. Xu, "Direct preparation of macro porous mullite supports for membranes by in situ reaction sintering," *Journal of Membrane Science*, vol. 318, no. 1, pp. 38–44, 2008.

[14] Z. Zhu, J. Xiao, W. He, T. Wang, Z. Wei, and Y. Dong, "A phase-inversion casting process for preparation of tubular

porous alumina ceramic membranes," *Journal of the European Ceramic Society*, vol. 35, no. 11, pp. 3187–3194, 2015.

[15] K. A. Defriend and A. R. Barron, "A simple approach to hierarchical ceramic ultrafiltration membranes," *Journal of Membrane Science*, vol. 212, no. 1-2, pp. 29–38, 2003.

[16] M. M. Lorente-Ayza, S. Mestre, M. Menéndez, and E. Sánchez, "Comparison of extruded and pressed low cost ceramic supports for microfiltration membranes," *Journal of the European Ceramic Society*, vol. 35, no. 13, pp. 3681–3691, 2015.

[17] A. R. Studart, U. T. Gonzenbach, E. Tervoort, and L. J. Gauckler, "Processing routes to macroporous ceramics: a review," *Journal of the American Ceramic Society*, vol. 89, no. 6, pp. 1771–1789, 2006.

[18] S. Khemakhem, A. Larbot, and R. B. Amar, "New ceramic microfiltration membranes from Tunisian natural materials: application for the cuttlefish effluents treatment," *Ceramics International*, vol. 35, no. 1, pp. 55–61, 2009.

[19] N. Kouras, A. Harabi, F. Bouzerara et al., "Macro-porous ceramic supports for membranes prepared from quartz sand and calcite mixtures," *Journal of the European Ceramic Society*, vol. 37, no. 9, pp. 3159–3165, 2017.

[20] D. Wang, A. Bao, W. Kunc, and W. Liss, "Coal power plant flue gas waste heat and water recovery," *Applied Energy*, vol. 91, no. 1, pp. 341–348, 2012.

[21] D. Wang, *Energy and Water Recovery with Transport Membrane Condenser*, Gas Technology Institute, Des Plaines, IL, USA, 2013.

[22] D. Wang, *Advanced Energy and Water Recovery Technology from Low Grade Waste Heat*, Gas Technology Institute, Des Plaines, IL, USA, 2011.

[23] D. Wang, *Transport Membrane Condenser for Water and Energy Recovery from Power Plant Flue Gas*, Institute of Gas Technology, Des Plaines, IL, USA, 2012.

[24] C. X. Lin, D. Wang, and A. Bao, "Numerical modeling and simulation of condensation heat transfer of a flue gas in a bundle of transport membrane tubes," *International Journal of Heat & Mass Transfer*, vol. 60, no. 60, pp. 41–50, 2013.

[25] A. Bao, D. Wang, and C. X. Lin, "Nanoporous membrane tube condensing heat transfer enhancement study," *International Journal of Heat & Mass Transfer*, vol. 84, pp. 456–462, 2015.

[26] T. Wang, M. Yue, H. Qi, P H.M. Feron, and S. Zhao, "Transport membrane condenser for water and heat recovery from gaseous streams: performance evaluation," *Journal of Membrane Science*, vol. 484, pp. 10–17, 2015.

[27] H. Chen, Y. Zhou, S. Cao et al., "Heat exchange and water recovery experiments of flue gas with using nanoporous ceramic membranes," *Applied Thermal Engineering*, vol. 110, pp. 686–694, 2016.

[28] Y. Zhou, H. Chen, T. Xie, B. Wang, and L. An, "Effect of mass transfer on heat transfer of microporous ceramic membranes for water recovery," *International Journal of Heat & Mass Transfer*, vol. 112, pp. 643–648, 2017.

[29] B. Ma, Y. Wu, and L. Liu, *Comprehensive Utilization of Fly Ash*, Science Press, Beijing, China, 2016.

[30] A. K. Saha and P. K. Sarker, "Sustainable use of ferronickel slag fine aggregate and fly ash in structural concrete: mechanical properties and leaching study," *Journal of Cleaner Production*, vol. 162, pp. 438–448, 2017.

[31] S. R. D. Silva and J. J. D. O. Andrade, "Investigation of mechanical properties and carbonation of concretes with construction and demolition waste and fly ash," *Construction & Building Materials*, vol. 153, pp. 704–715, 2017.

[32] M. Hermassi, C. Valderrama, N. Moreno et al., "Fly ash as reactive sorbent for phosphate removal from treated waste water as a potential slow release fertilizer," *Journal of Environmental Chemical Engineering*, vol. 5, no. 1, pp. 160–169, 2017.

[33] N. Kabay, M. M. Tufekci, A. B. Kizilkanat, and D. Oktay, "Properties of concrete with pumice powder and fly ash as cement replacement materials," *Construction & Building Materials*, vol. 85, pp. 1–8, 2015.

[34] J. Yu, C. Lu, C. K. Y. Leung, and G. Li, "Mechanical properties of green structural concrete with ultrahigh-volume fly ash," *Construction & Building Materials*, vol. 147, pp. 510–518, 2017.

[35] M. A. Ozdemir, "Improvement in bearing capacity of a soft soil by addition of fly ash," *Procedia Engineering*, vol. 143, pp. 498–505, 2016.

[36] S. M. Shaheen, P. S. Hooda, and C. D. Tsadilas, "Opportunities and challenges in the use of coal fly ash for soil improvements—a review," *Journal of Environmental Management*, vol. 145, pp. 249–267, 2014.

[37] N. L. Ukwattage, P. G. Ranjith, and M. Bouazza, "The use of coal combustion fly ash as a soil amendment in agricultural lands (with comments on its potential to improve food security and sequester carbon)," *Fuel*, vol. 109, no. 7, pp. 400–408, 2013.

[38] Z. T. Yao, X. S. Ji, P. K. Sarker et al., "A comprehensive review on the applications of coal fly ash," *Earth-Science Reviews*, vol. 141, no. 141, pp. 105–121, 2015.

[39] J. Cao, X. Dong, L. Li, Y. Dong, and S. Hampshire, "Recycling of waste fly ash for production of porous mullite ceramic membrane supports with increased porosity," *Journal of the European Ceramic Society*, vol. 34, no. 13, pp. 3181–3194, 2014.

[40] Y. Dong, X. Liu, Q. Ma, and G. Meng, "Preparation of cordierite-based porous ceramic micro-filtration membranes using waste fly ash as the main raw materials," *Journal of Membrane Science*, vol. 285, no. 1, pp. 173–181, 2006.

[41] X. Wu, Z. Huo, Q. Ren, H. Li, F. Lin, and T. Wei, "Preparation and characterization of ceramic proppants with low density and high strength using fly ash," *Journal of Alloys & Compounds*, vol. 702, pp. 442–448, 2017.

[42] J. Fang, G. Qin, W. Wei, and X. Zhao, "Preparation and characterization of tubular supported ceramic microfiltration membranes from fly ash," *Separation & Purification Technology*, vol. 80, no. 3, pp. 585–591, 2011.

[43] J. Liu, Y. Dong, X. Dong et al., "Feasible recycling of industrial waste coal fly ash for preparation of anorthite-cordierite based porous ceramic membrane supports with addition of dolomite," *Journal of the European Ceramic Society*, vol. 36, no. 4, pp. 1059–1071, 2016.

[44] F. Yang, C. Li, Y. Lin, and C-A. Wang, "Effects of sintering temperature on properties of porous mullite/corundum ceramics," *Materials Letters*, vol. 73, pp. 36–39, 2012.

[45] G. Pia, L. Casnedi, and U. Sanna, "Porous ceramic materials by pore-forming agent method: an intermingled fractal units analysis and procedure to predict thermal conductivity," *Ceramics International*, vol. 41, no. 5, pp. 6350–6357, 2015.

[46] J. Zhou, Y. Yang, Q. Chang, Y. Wang, K. Yang, and Q. Bao, "Effect of particle size on the pore size and flexural strength of alumina porous ceramic membrane support," *Journal of Synthetic Crystals*, vol. 43, no. 8, pp. 2125–2131, 2014.